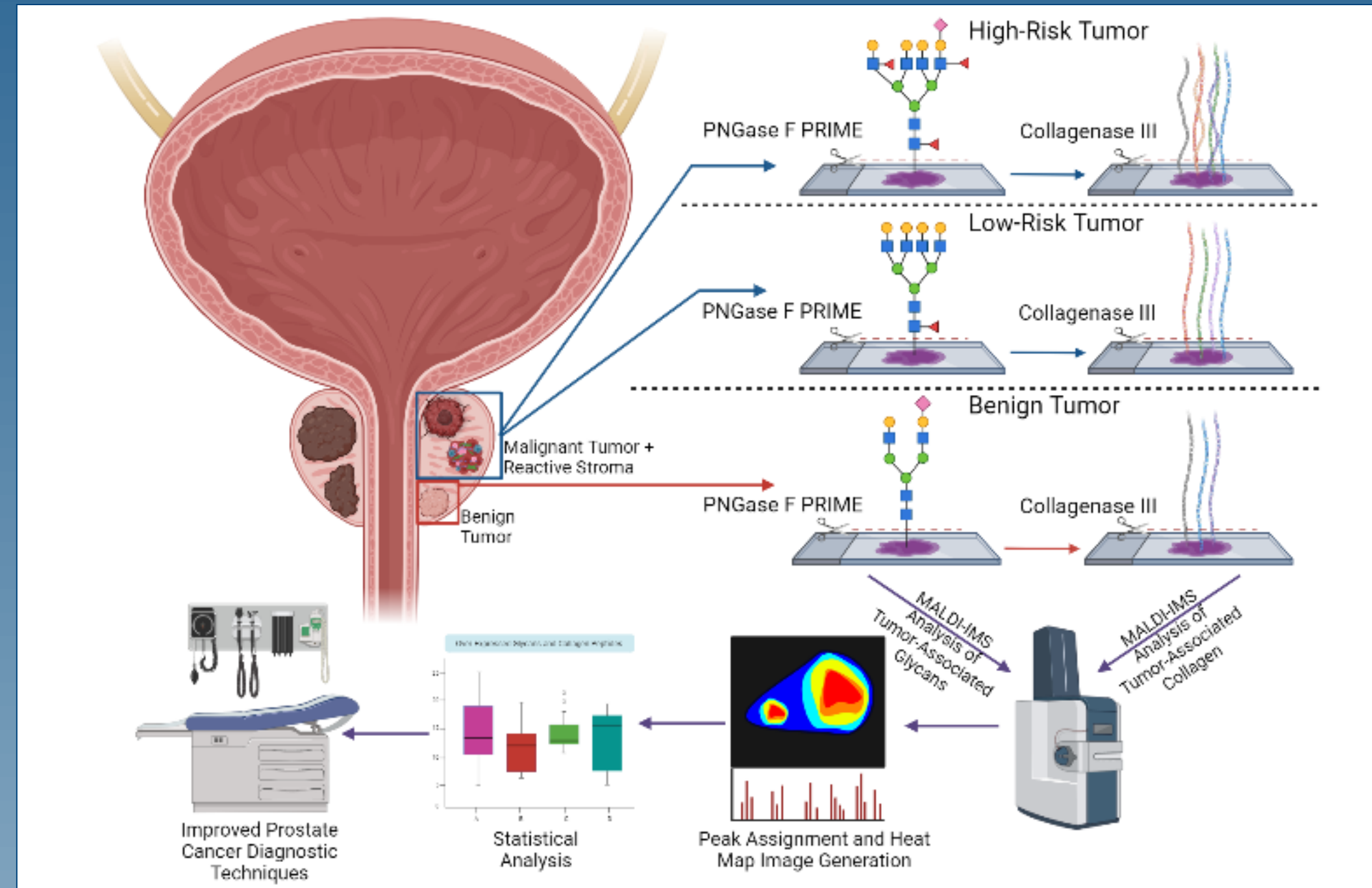


# Establishment of the Full Glycan and Collagen Biomarker Profile for Prostate Cancer Tissue Samples Representing a Broad Spectrum of Histopathologies Using MALDI-IMS

Jordan Hartig<sup>1</sup>, Peggi Angel<sup>1</sup>, Lydia Liu<sup>2</sup>, Amanda Khoo<sup>2</sup>, Stan Liu<sup>3</sup>, Michelle Downs<sup>3</sup>, Paul Boutros<sup>4</sup>, Thomas Kislinger<sup>2</sup>, Richard Drake<sup>1</sup>

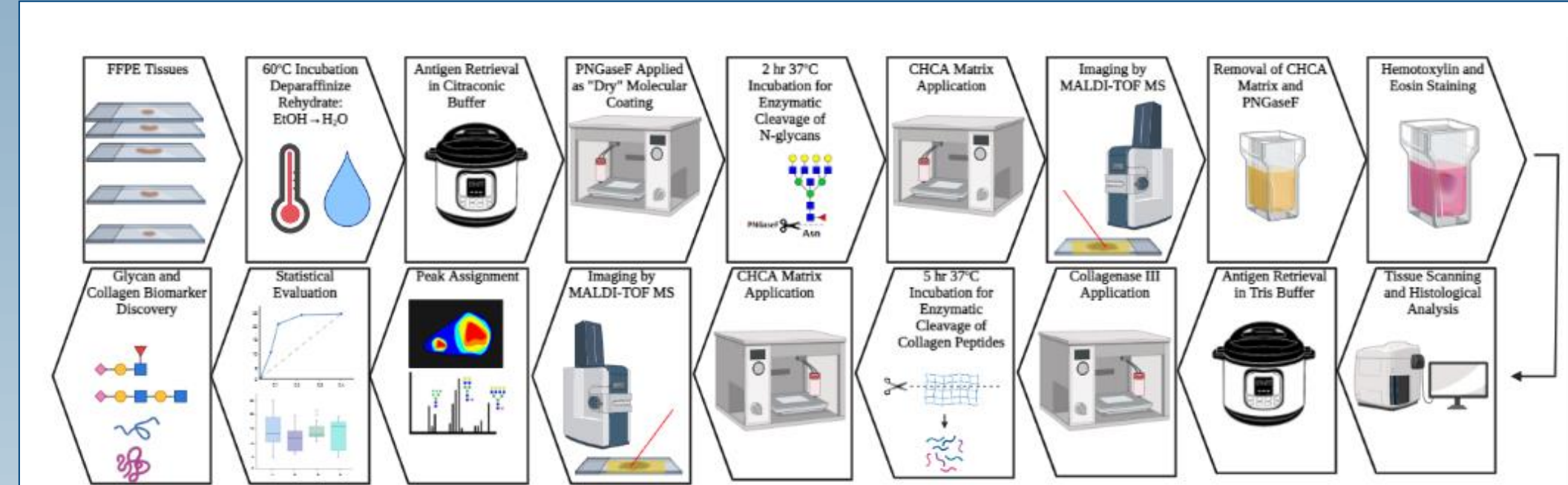
<sup>1</sup>Medical University of South Carolina, Charleston, SC  
<sup>2</sup>Princess Margaret Cancer Centre, University of Toronto, Toronto, ON  
<sup>3</sup>Sunnybrook Health Science Centre, Toronto, ON  
<sup>4</sup>University of California Los Angeles, Los Angeles, CA

## BACKGROUND



**Figure 1:** Prostate Cancer is characterized by changes in glycosylation and the emergence of reactive stroma. This study aims to analyze these changes via MALDI-IMS to improve Prostate Cancer diagnostic techniques. Created with BioRender.com

## METHODS



Tumor Gleason Score	Number of Tissues	Number of Different Histopathologies			
Gleason 4	45	Glomeruloid: 4	Cribriform: 20	Fused: 20	PFG: 11 IDC: 2
Gleason 5	38	Solid: 26		Single: 17	Necrosis: 3
Other Malignant	8	IDC: 6	Gleason 3: 1	Ductal: 1	
Benign	40				

**Figure 2:** (Top) Tissue preparation and analysis workflow. Created with BioRender.com. Each tissue was processed for N-glycan MALDI-IMS by digestion with PNGase F PRIME. Following N-glycan and matrix removal, collagenase digestion and further MALDI-IMS detection of ECM peptides was performed. Data was processed using SCI LS and Microsoft Excel. H&E Staining was performed for histological analysis. (Bottom) Chart detailing the histopathological distribution of tumors within the cohort. Total number of tissues is 112

## N-GLYCAN DISTRIBUTION IN GLEASON 4 COHORT

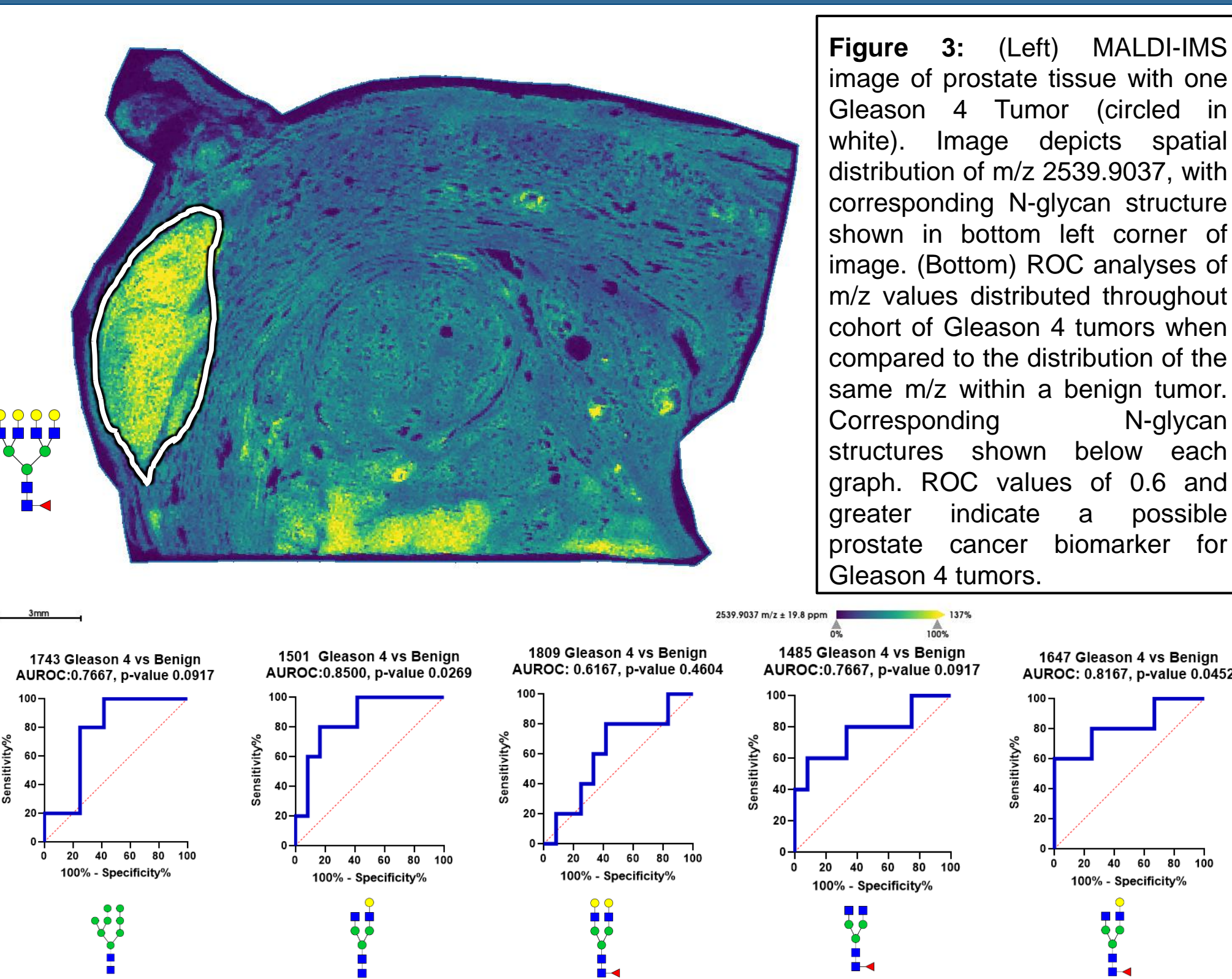


**Figure 3:** (Left) MALDI-IMS image of prostate tissue with one Gleason 4 Tumor (circled in white). Image depicts spatial distribution of m/z 2539.9037, with corresponding N-glycan structure shown in bottom left corner of image. (Bottom) ROC analyses of m/z values distributed throughout cohort of Gleason 4 tumors when compared to the distribution of the same m/z within a benign tumor. Corresponding N-glycan structures shown below each graph. ROC values of 0.6 and greater indicate a possible prostate cancer biomarker for Gleason 4 tumors.

## N-GLYCAN DISTRIBUTION IN GLEASON 5 COHORT

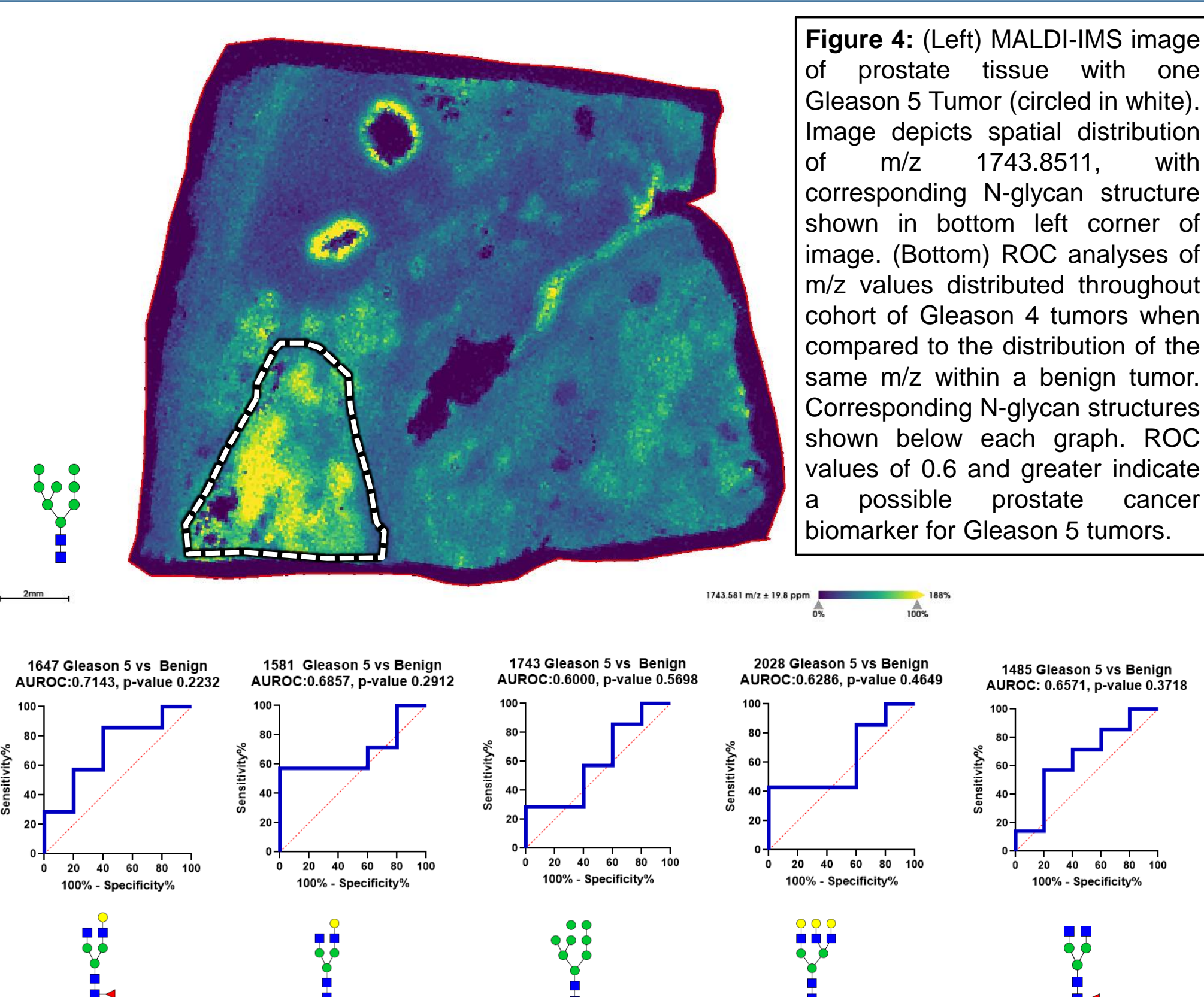


**Figure 4:** (Left) MALDI-IMS image of prostate tissue with one Gleason 5 Tumor (circled in white). Image depicts spatial distribution of m/z 1743.8511, with corresponding N-glycan structure shown in bottom left corner of image. (Bottom) ROC analyses of m/z values distributed throughout cohort of Gleason 4 tumors when compared to the distribution of the same m/z within a benign tumor. Corresponding N-glycan structures shown below each graph. ROC values of 0.6 and greater indicate a possible prostate cancer biomarker for Gleason 5 tumors.

## STROMA-ASSOCIATED N-GLYCANS

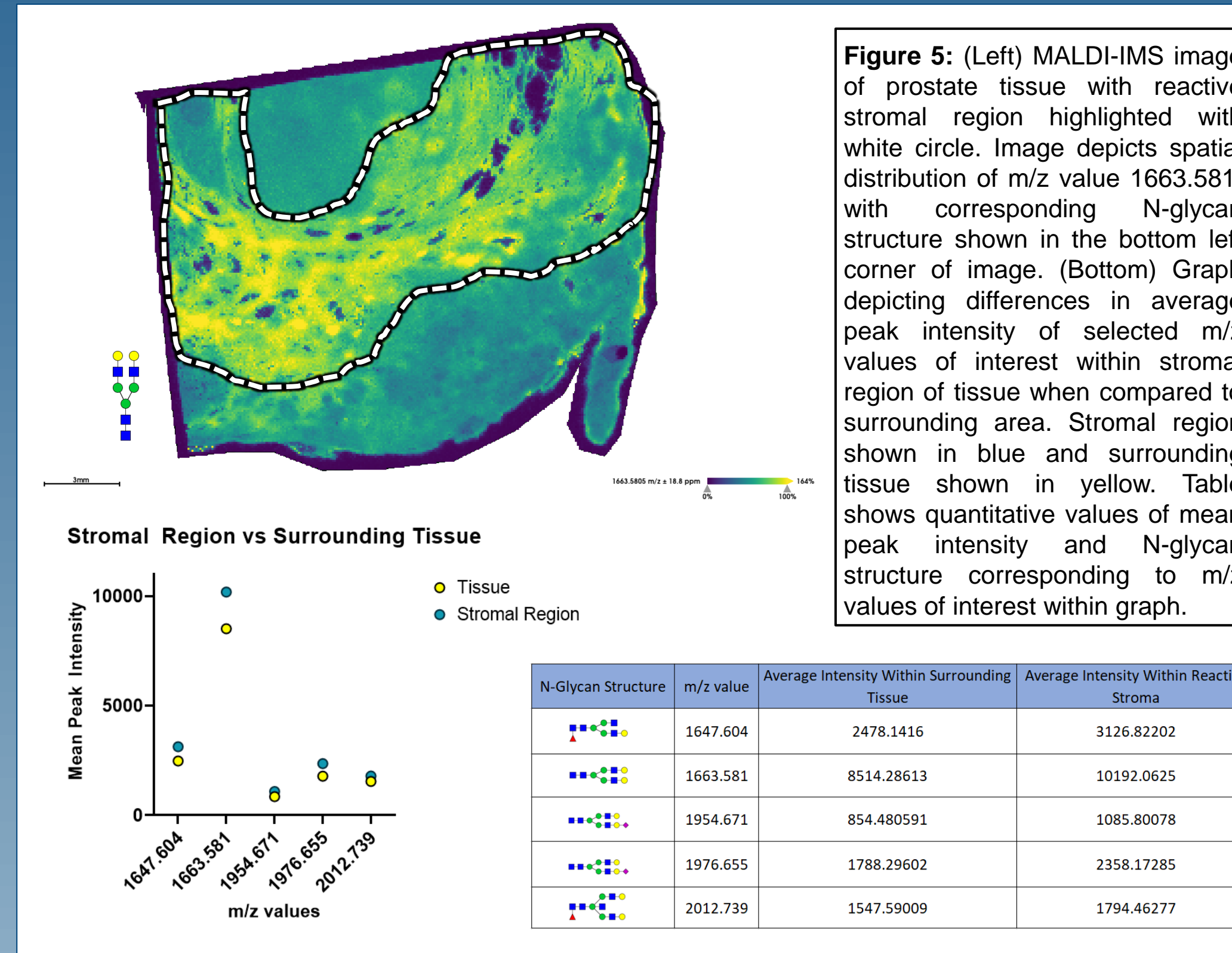


**Figure 5:** (Left) MALDI-IMS image of prostate tissue with reactive stromal region highlighted with white circle. Image depicts spatial distribution of m/z value 1663.581, with corresponding N-glycan structure shown in the bottom left corner of image. (Bottom) Graph depicting differences in average peak intensity of selected m/z values of interest within stromal region of tissue when compared to surrounding area. Stromal region shown in blue and surrounding tissue shown in yellow. Table shows quantitative values of mean peak intensity and N-glycan structure corresponding to m/z values of interest within graph.

## N-GLYCAN DISTRIBUTION IN OTHER MALIGNANCIES

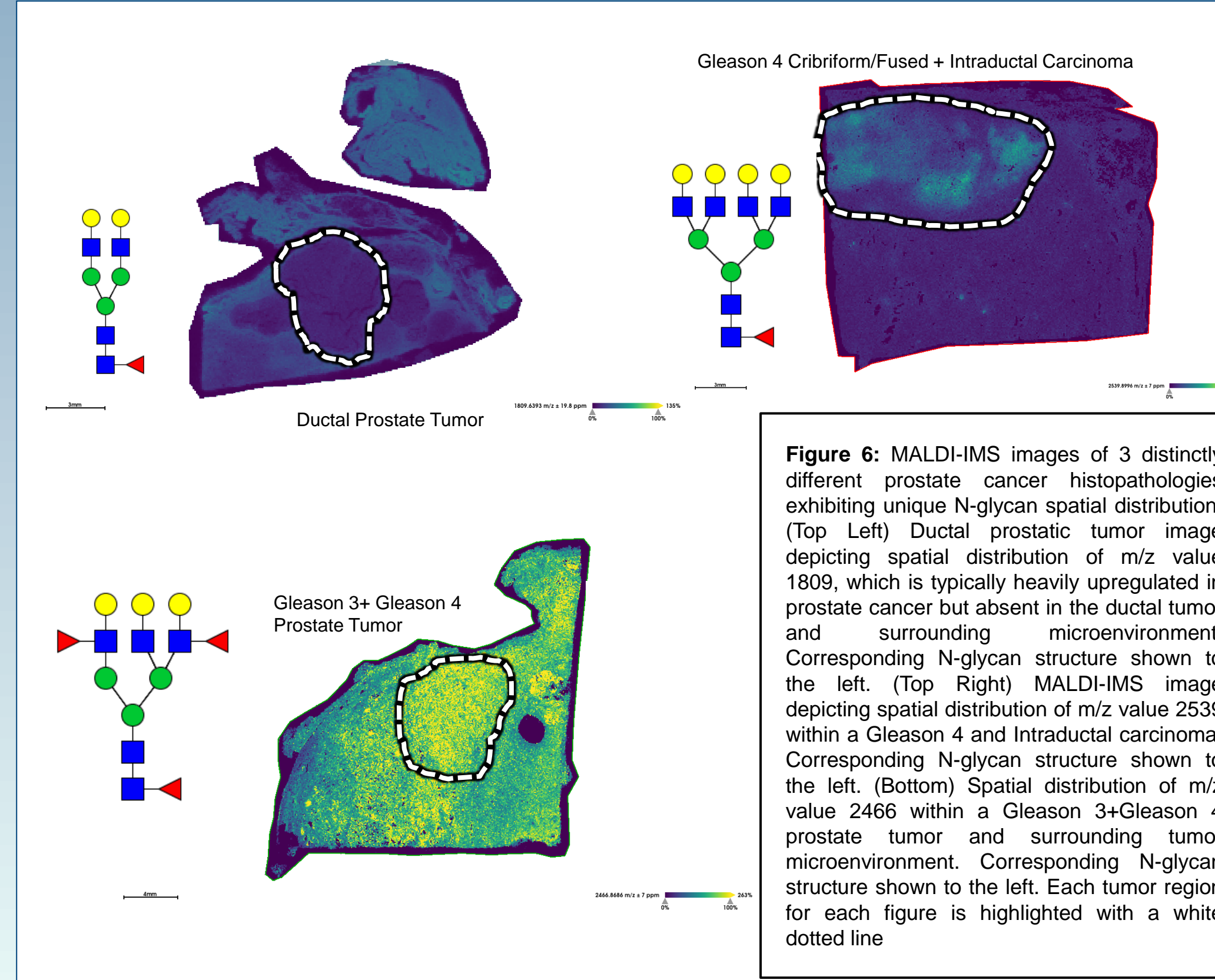


**Figure 6:** MALDI-IMS images of 3 distinctly different prostate cancer histopathologies exhibiting unique N-glycan spatial distribution. (Top Left) Ductal prostatic tumor image depicting spatial distribution of m/z value 1809, which is typically heavily upregulated in prostate cancer but absent in the ductal tumor and surrounding microenvironment. Corresponding N-glycan structure shown to the left. (Top Right) MALDI-IMS image depicting spatial distribution of m/z value 2539 within a Gleason 4 and Intraductal carcinoma. Corresponding N-glycan structure shown to the left. (Bottom) Spatial distribution of m/z value 2466 within a Gleason 3+Gleason 4 prostate tumor and surrounding tumor microenvironment. Corresponding N-glycan structure shown to the left. Each tumor region for each figure is highlighted with a white dotted line

## COLLAGEN ANALYSIS OF COHORT

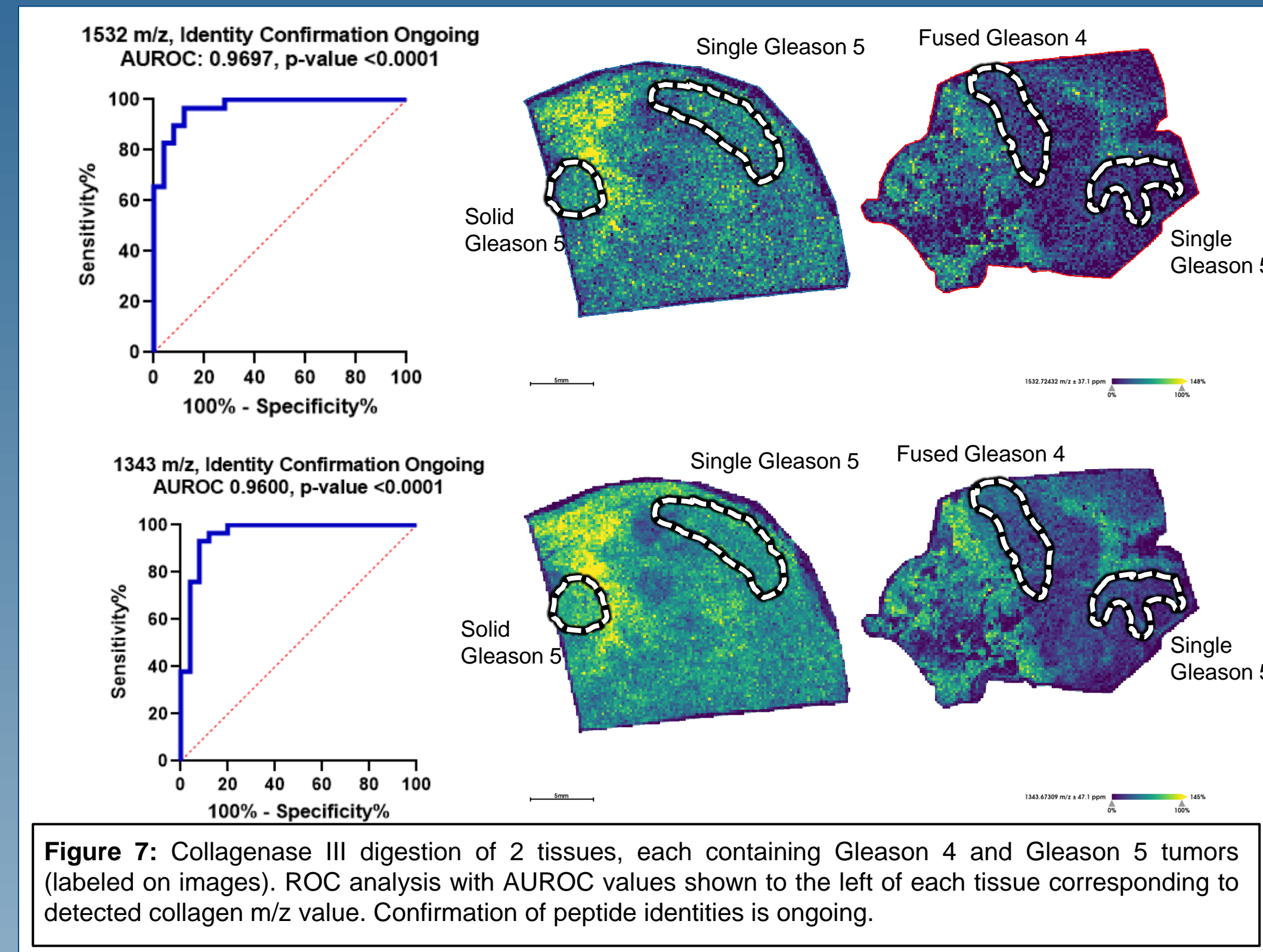


**Figure 7:** Collagenase III digestion of 2 tissues, each containing Gleason 4 and Gleason 5 tumors (labeled on images). ROC analysis with AUROC values shown to the left of each tissue corresponding to detected collagen m/z value. Confirmation of peptide identities is ongoing.

## CONCLUSION

- A multi-enzymatic approach was used to understand the N-glycan and collagen composition of prostatic tumors
- Major tumor-associated N-glycans fall within the high-mannose and pauci-mannose categories
- Multiple branched N-glycan species with different combinations of fucose and sialic acid constituents were also associated with tumor incidence and progression
- A subset of branched N-glycans were associated with higher intensities in tumors with higher Gleason scores
- Additional proteomic studies are ongoing with the goal of evaluating identity and prevalence of ECM and collagen peptide distribution in correlation with different tumor subtypes
- Analyses to evaluate N-glycan isomer distributions for fucosylated and sialylated N-glycan species are also ongoing

## REFERENCES

• Mapping Extracellular Matrix Proteins in Formalin-Fixed, Paraffin-Embedded Tissues by MALDI Imaging Mass Spectrometry, Peggi M. Angel, Susana Comte-Walters, Lauren E. Ball, Kacey Talbot, Anand Mehta, Kelvin G.M Brockbank, and Richard R. Drake. *Journal of Proteome Research* 2018 17 (1), 635-646 DOI: 10.1021/acs.jproteome.7b00713

• Angel P.M., Mehta A., Norris-Caneda K., Drake R.R. (2017) MALDI Imaging Mass Spectrometry of N-glycans and Tryptic Peptides from the Same Formalin-Fixed, Paraffin-Embedded Tissue Section. In: Sarwal M., Sigdel T. (eds) *Tissue Proteomics. Methods in Molecular Biology*, vol 1788. Humana Press, New York, NY.

• Scott, E. and J. Munkley (2019). Glycans as biomarkers in prostate cancer. *International Journal of Molecular Sciences*, MDPI AG. 20.

## ACKNOWLEDGMENTS

This work is funded by NIH R01 CA212409

**Contact:**  
Jordan Paige Hartig  
PhD Student, Drake Lab  
Medical University of South Carolina  
hartig@muscu.edu